Polarization-independent chalcogenide glass nanowires with anomalous dispersion for all-optical processing

Xin Gai,[*] Duk-Yong Choi, Steve Madden, and Barry Luther-Davies

Centre for Ultrahigh-bandwidth Devices for Optical Systems (CUDOS), Laser Physics Centre, Research School of Physics and Engineering, Australian National University, Canberra ACT2600, Australia

[*]*xga111@rsphysse.anu.edu.au*

Abstract: We demonstrate the design and fabrication of square $Ge_{11.5}As_{24}Se_{64.5}$ (Ge_{11}) nonlinear nanowires fully embedded in a silica cladding for polarization independent (P-I) nonlinear processing. We observed similar performance for FWM using both TE and TM modes confirming that a near P-I operation was obtained. In addition we find that the supercontinuum spectrum that can be generated in the nanowires using 1ps pulse pulses with around 30W peak power was independent of polarization.

OCIS codes: (130.2755) Glass waveguides; (220.0220) Optical design and fabrication; (190.4410) Nonlinear optics, parametric processes.

References and links

1. J. T. Gopinath, M. Soljacic, E. P. Ippen, V. N. Fuflyigin, W. A. King, and M. Shurgalin, "Third order nonlinearities in Ge-As-Se-based glasses for telecommunications applications," J. Appl. Phys. **96**(11), 6931–6933 (2004).
2. J. M. Harbold, F. O. Ilday, F. W. Wise, and B. G. Aitken, "Highly nonlinear Ge-As-Se and Ge-As-S-Se glasses for all-optical switching," IEEE Photon. Technol. Lett. **14**(6), 822–824 (2002).
3. A. Prasad, C. J. Zha, R. P. Wang, A. Smith, S. Madden, and B. Luther-Davies, "Properties of GexAsySe1-x-y glasses for all-optical signal processing," Opt. Express **16**(4), 2804–2815 (2008).
4. A. Prasad, "Ge-As-Se chalcogenide glasses for all-optical signal processing," in *Laser Physics Center*(Australian National University, 2010).
5. M. R. E. Lamont, B. Luther-Davies, D. Y. Choi, S. Madden, X. Gai, and B. J. Eggleton, "Net-gain from a parametric amplifier on a chalcogenide optical chip," Opt. Express **16**(25), 20374–20381 (2008).
6. F. Luan, M. D. Pelusi, M. R. E. Lamont, D. Y. Choi, S. Madden, B. Luther-Davies, and B. J. Eggleton, "Dispersion engineered As(2)S(3) planar waveguides for broadband four-wave mixing based wavelength conversion of 40 Gb/s signals," Opt. Express **17**(5), 3514–3520 (2009).
7. M. D. Pelusi, F. Luan, S. Madden, D. Y. Choi, D. A. Bulla, B. Luther-Davies, and B. J. Eggleton, "Wavelength Conversion of High-Speed Phase and Intensity Modulated Signals Using a Highly Nonlinear Chalcogenide Glass Chip," IEEE Photon. Technol. Lett. **22**(1), 3–5 (2010).
8. M. Galili, J. Xu, H. C. H. Mulvad, L. K. Oxenløwe, A. T. Clausen, P. Jeppesen, B. Luther-Davis, S. Madden, A. Rode, D. Y. Choi, M. Pelusi, F. Luan, and B. J. Eggleton, "Breakthrough switching speed with an all-optical chalcogenide glass chip: 640 Gbit/s demultiplexing," Opt. Express **17**(4), 2182–2187 (2009).
9. T. D. Vo, H. Hu, M. Galili, E. Palushani, J. Xu, L. K. Oxenløwe, S. J. Madden, D. Y. Choi, D. A. P. Bulla, M. D. Pelusi, J. Schröder, B. Luther-Davies, and B. J. Eggleton, "Photonic chip based transmitter optimization and receiver demultiplexing of a 1.28 Tbit/s OTDM signal," Opt. Express **18**(16), 17252–17261 (2010).
10. M. D. Pelusi, F. Luan, D. Y. Choi, S. J. Madden, D. A. P. Bulla, B. Luther-Davies, and B. J. Eggleton, "Optical phase conjugation by an As(2)S(3) glass planar waveguide for dispersion-free transmission of WDM-DPSK signals over fiber," Opt. Express **18**(25), 26686–26694 (2010).
11. G. P. Agrawal, *Nonlinear Fiber Optics,* (Academic Press Inc., 2001).
12. W. R. Headley, G. T. Reed, S. Howe, A. Liu, and M. Paniccia, "Polarization-independent optical racetrack resonators using rib waveguides on silicon-on-insulator," Appl. Phys. Lett. **85**(23), 5523–5525 (2004).
13. X. Chen and H. K. Tsang, "Polarization-independent grating couplers for silicon-on-insulator nanophotonic waveguides," Opt. Lett. **36**(6), 796–798 (2011).
14. S. M. Gao, X. Z. Zhang, Z. Q. Li, and S. L. He, "Polarization-Independent Wavelength Conversion Using an Angled-Polarization Pump in a Silicon Nanowire Waveguide," IEEE J. Sel. Top. Quantum. Electron. **16**(1), 250–256 (2010).

#167778 - $15.00 USD Received 1 May 2012; revised 22 May 2012; accepted 24 May 2012; published 1 Jun 2012

15. Y. Tian, P. Dong, and C. X. Yang, "Polarization independent wavelength conversion in fibers using incoherent pumps," Opt. Express **16**(8), 5493–5498 (2008).
16. S. P. Chan, C. E. Phun, S. T. Lim, G. T. Reed, and V. M. N. Passaro, "Single-mode and polarization-independent silicon-on-insulator waveguides with small cross section," J. Lightwave Technol. **23**(6), 2103–2111 (2005).
17. S. T. Lim, C. E. Png, E. A. Ong, and Y. L. Ang, "Single mode, polarization-independent submicron silicon waveguides based on geometrical adjustments," Opt. Express **15**(18), 11061–11072 (2007).
18. X. Gai, D. Y. Choi, S. Madden, and B. Luther-Davies, "Interplay between Raman scattering and four-wave mixing in As(2)S(3) chalcogenide glass waveguides," J. Opt. Soc. Am. B **28**(11), 2777–2784 (2011).
19. X. Gai, S. Madden, D. Y. Choi, D. Bulla, and B. Luther-Davies, "Dispersion engineered Ge(11.5)As(24)Se(64.5) nanowires with a nonlinear parameter of 136 $W^{(-1)}m^{(-1)}$ at 1550 nm," Opt. Express **18**(18), 18866–18874 (2010).
20. A. B. Fallahkhair, K. S. Li, and T. E. Murphy, "Vector finite difference modesolver for anisotropic dielectric waveguides," J. Lightwave Technol. **26**(11), 1423–1431 (2008).
21. P. Lusse, P. Stuwe, J. Schule, and H. G. Unger, "Analysis of Vectorial Mode Fields in Optical Wave-Guides by a New Finite-Difference Method," J. Lightwave Technol. **12**(3), 487–494 (1994).
22. C. Koos, L. Jacome, C. Poulton, J. Leuthold, and W. Freude, "Nonlinear silicon-on-insulator waveguides for all-optical signal processing," Opt. Express **15**(10), 5976–5990 (2007).
23. X. Gai, R. P. Wang, C. Xiong, M. J. Steel, B. J. Eggleton, and B. Luther-Davies, "Near-zero anomalous dispersion Ge11.5As24Se64.5 glass nanowires for correlated photon pair generation: design and analysis," Opt. Express **20**(2), 776–786 (2012).
24. D. Y. Choi, S. Madden, A. Rode, R. P. Wang, A. Ankiewicz, and B. Luther-Davies, "Surface roughness in plasma-etched As2S3 films: Its origin and improvement," IEEE T. Nanotechnol. **7**(3), 285–290 (2008).
25. J. J. Hu, N. N. Feng, N. Carlie, L. Petit, J. F. Wang, A. Agarwal, K. Richardson, and L. Kimerling, "Low-loss high-index-contrast planar waveguides with graded-index cladding layers," Opt. Express **15**(22), 14566–14572 (2007).
26. Q. Lin and G. P. Agrawal, "Vector theory of four-wave mixing: polarization effects in fiber-optic parametric amplifiers," J. Opt. Soc. Am. B **21**(6), 1216–1224 (2004).

1. Introduction

Recently, nonlinear waveguides fabricated from chalcogenide glasses have been shown to be excellent materials for all-optical processing due to their attractive optical properties which include good light confinement as a result of their high refractive index; high nonlinear refractive index, n_2 [1–3]; and negligible two photon (TPA) and free carrier absorption (FCA) at telecommunications frequencies [2, 4]. Many all-optical processes have now been demonstrated using dispersion-engineered As_2S_3 chalcogenide rib waveguides including parametric amplification [5]; wavelength conversion [6, 7]; Tb/s demultiplexing [8, 9]; and dispersion compensation by mid-span spectral inversion [10]. Most of these functions involved four wave mixing (FWM) which becomes efficient when phase matching is achieved according to the condition: $-4\gamma P<\beta_2\Delta\omega^2<0$, where $\gamma = 2\pi n_2/\lambda A_{eff}$ is the nonlinear parameter of the waveguide; P is the peak pump power; β_2 is the second order dispersion; and $\Delta\omega$ is the difference between pump and signal frequencies. According to this phase matching relation, the waveguides need to have small and anomalous dispersion ($\beta_2\leq 0$) to achieve exponential gain from FWM [11]. However, in a typical dispersion-engineered As_2S_3 rib waveguide only one polarization state, the transverse magnetic mode (TM), exhibits anomalous dispersion whilst the transverse electric mode (TE) has a large normal dispersion that does not support FWM except over a vanishingly small bandwidth. Since light from a fiber is normally polarized randomly, the polarization-dependent dispersion of an As_2S_3 rib waveguide means that both pump and signal waves must be adjusted to have the same polarization state and this requires many additional components to convert the light into the TM mode. This is undesirable for integrated optical circuits and impractical for commercial applications in fiber communication networks. As a result, structures that would allow FWM of randomly polarized signal beams in polarization-insensitive waveguides are of significant interest.

There have been several reports aimed at achieving polarization-independent (P-I) devices, e.g. P-I racetrack resonators [12]; P-I grating couplers [13]; P-I wavelength convertors [14, 15]; and P-I waveguides [16, 17]. However, most of these studies focused on devices made from the silicon-on-insulator (SOI) platform where, in general, the silicon film

#167778 - $15.00 USD Received 1 May 2012; revised 22 May 2012; accepted 24 May 2012; published 1 Jun 2012

thickness is not a free parameter. By comparison, there have been no studies of P-I chalcogenide glass waveguides. Furthermore, in previous work, the P-I waveguides were designed to operate at a fixed wavelength and the geometry of an asymmetric waveguide – its width, thickness and etch depth – was varied to find a crossing point where the effective index, n_{eff}, of the TM and TE modes were the same so that zero birefringence could be obtained [16, 17]. However, this kind of structure maintains zero birefringence only over a very narrow bandwidth because n_{eff} will change with frequency due to material and waveguide dispersion. Furthermore, zero birefringence indicates little about the relative values of β_2 for the TE and TM modes, which due to the structural asymmetry, will almost certainly be different. Since β_2 affects the bandwidth and shape of FWM gain spectrum, this can result in a very different FWM behavior between the TM and TE modes [18]. Therefore, waveguides with P-I dispersion are required for all-optical processing.

Two conditions are required to achieve a waveguide with P-I dispersion suitable for FWM. Firstly, the structure should be symmetric since this is the most straightforward way to both eliminate birefringence and to achieve the same dispersion in both the TM and TE modes. This requires a waveguide with square cross-section embedded in a uniform cladding. Secondly, because most chalcogenide glasses exhibit very high normal material dispersion at telecommunications wavelengths, large anomalous waveguide dispersion is required to compensate the material dispersion and achieve a net dispersion that is small and anomalous. However, square waveguides with dimensions of a few microns do not create enough anomalous waveguide dispersion because the fundamental modes are too tightly confined within the core. In order to increase the anomalous waveguide dispersion, sub-micron nanowires are, therefore, required. It is also beneficial if the waveguide is very short since this minimizes the effects of any residual polarization-dependent loss, residual birefringence or any difference in the dispersion caused by fabrication errors. Since any nonlinear process requires some minimum nonlinear phase change to achieve adequate efficiency, a high nonlinear parameter γ is then essential and this can be achieved using a nanowire.

In our previous work we have shown that $Ge_{11.5}As_{24}Se_{64.5}$ (Ge_{11}) chalcogenide glass which has nonlinear index three times more than that of As_2S_3 [3] can be used to make nanowires with a high nonlinear parameter γ of up to $136W^{-1}m^{-1}$ [19] which is more than ten times of that of As_2S_3 rib waveguides [5–10]. Compared with 6cm long As_2S_3 waveguides widely used in our previous work a Ge_{11} nanowire only has to be ≈0.5cm long to obtain the same nonlinear response. Assuming a difference of 10ps/km/nm in the group velocity dispersion (GVD) between the TM and TE modes arises from fabrication errors, only 0.5×10^{-5}ps/nm dispersion difference will be induced and this implies that polarization-independence can be achieved over a very broad bandwidth.

In this paper, we report, on the fabrication and properties of square Ge_{11} nonlinear nanowires fully embedded in a silica cladding. We measure their performance for FWM using both TE and TM modes to confirm that a near P-I operation was obtained. In addition we demonstrate that the supercontinuum spectrum that can be generated in the waveguides using 1ps pulse pulses with around 30W peak power was independent of polarization.

2. Design and fabrication of P-I nanowires

In order to obtain a high nonlinear parameter γ in the nanowires, we need to minimize the effective area A_{eff} of the waveguide mode. The mode intensity distribution is shown in Figs. 1(a) and 1(b) for TM and TE polarizations respectively. Figure 1(c) shows the effective area as a function of waveguide dimension for a square Ge_{11} nanowire fully embedded in a SiO_2 cladding at 1550nm with the eigenvalues and mode distribution calculated by the FDTD method [20, 21] with the effective area defined as in [22]. The effective area increases exponentially when the waveguide dimension drops below 0.4μm because the core-cladding index difference (≈1.2) cannot confine a smaller mode. In comparison, nanowires with

#167778 - $15.00 USD Received 1 May 2012; revised 22 May 2012; accepted 24 May 2012; published 1 Jun 2012

dimensions between 0.4μm and 0.6μm achieve the smallest effective area ranging from $0.25\mu m^2$ to $0.28\mu m^2$ and this is, therefore, the range that we concentrated on.

In this range, as would be expected, the same anomalous dispersion is obtained for both TM and TE modes at 1550nm and a GVD of 165ps/km/nm is predicted for a 580nm × 580nm nanowire as show in Fig. 1(d). Although a smaller near-zero dispersion is preferred in most all-optical devices because it gives a broad bandwidth for FWM and reduces distortion on the pulses during propagation, this is not a problem for Ge_{11} nanowires because only a short device is required to obtain sufficient nonlinear response. In fact, a 0.5cm long Ge_{11} nanowire with GVD of 165ps/km/nm will lead to only about the half dispersive phase shift compared with a 6cm As_2S_3 rib waveguide with GVD of 30ps/km/nm, and this implies a wider bandwidth can be achieved with less dispersive distortion of the pulses. Since the As_2S_3 ribs waveguide already demonstrated a FWM bandwidth in excess of 10THz, the higher dispersion is, therefore, of no concern. On the other hand, the high anomalous dispersion leads to a very short soliton fission length which is critical for supercontinuum (SC) generation and allows SC to be created in a very short device. The effective index n_{eff} and nonlinear parameter γ are shown in Fig. 1(e) and Fig. 1(f) respectively, which indicate the nonlinear parameter of ~130 $W^{-1}m^{-1}$ is achievable at 1550nm.

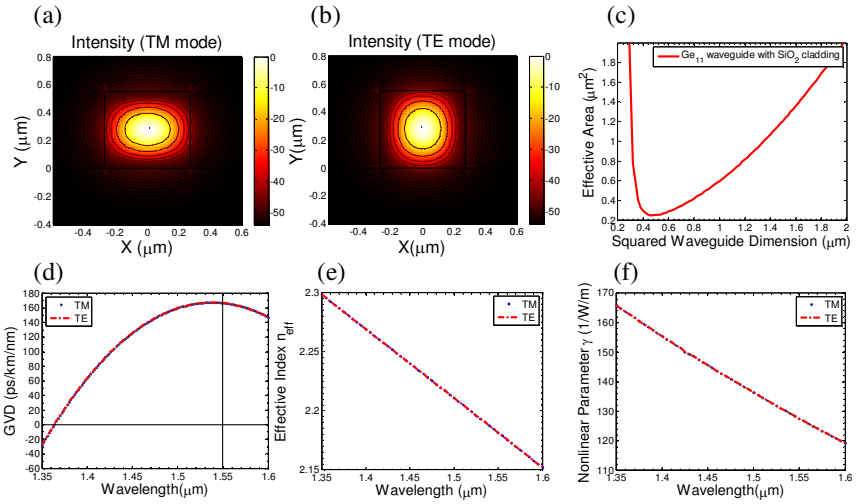

Fig. 1. Design of square Ge_{11} nanowires full embedded in SiO_2. (a) Intensity distribution for TM mode. (b) Intensity distribution for TE mode. (c) The effective area A_{eff} as a function of the waveguide dimensions. (d) GVD for 580nm × 580nm Ge_{11} nanowires. (e) Effective index n_{eff} for 580nm × 580nm Ge_{11} nanowires. (f) Nonlinear parameter γ for 580nm × 580nm Ge_{11} nanowires. Blue dots are the TM mode and the red line is for TE mode.

The nanowires were fabricated using the following process. Firstly, a 580nm Ge_{11} film was deposited onto an oxidized silicon wafer by thermal evaporation. A 200nm thick layer ZEP was then spin-coated onto the Ge_{11} film as the e-beam resist. E-beam lithography (EBL) was used to transfer the nanowire pattern onto the ZEP using the fixed beam moving stage method (FBMS) in which the electron beam is scanned over a small area whilst the stage is moved simultaneously to draw the pattern. By using FBMS the stitching errors between different writing fields in EBL were eliminated which helps reduce the loss of the nanowires. Inductively coupled plasma dry etching (Plasmalab system 100) was applied to transfer the pattern into the Ge_{11} film and the residual resist was removed by oxygen plasma. At the end of the process, about 1.5μm of SiO_2 was coated onto the nanowires as the top cladding using ion sputtering. "Snake" structures were also fabricated to integrate longer nanowires on the small chips as shown in Fig. 2(a) and to allow loss measurements by the "cut-back" method. The bend radius was 20μm for which modeling predicted the bending loss to be negligible.

#167778 - $15.00 USD Received 1 May 2012; revised 22 May 2012; accepted 24 May 2012; published 1 Jun 2012

Figure 2(b) shows SEM images of the profile of the resulting Ge_{11} nanowires. The square nanowires were well defined with near vertical side-walls. The nanowire width was measured to be 584nm and the height 575nm. Therefore, the fabrication error was controlled under ± 5nm, which is less than one percent of the nanowire dimension. In order to analyze the mismatch of n_{eff} and GVD between the TM and TE modes due to the fabrication errors, we calculated the n_{eff} and GVD for 585nm × 575nm nanowires as shown in Fig. 2(c) and 2(d). The difference in n_{eff} and GVD is predicted to be 0.004 and 1.7ps/km/nm at 1550nm respectively. Assuming a 5mm long device these differences have a negligible effect on nonlinear processes such as FWM. The loss of nanowires was measured to be 1.65dB/cm and 2.2dB/cm for TM and TE modes respectively by the cut-back method using three different waveguide lengths: 0.7cm, 1.2cm and 1.7cm (Fig. 2(e)). The coupling loss was 6dB at each facet. As a result, only 0.28 dB difference in the loss will be introduced over a 5mm long nanowire which is small enough not to affect the polarization of the propagating beams although lower PDL would be desirable in longer devices.

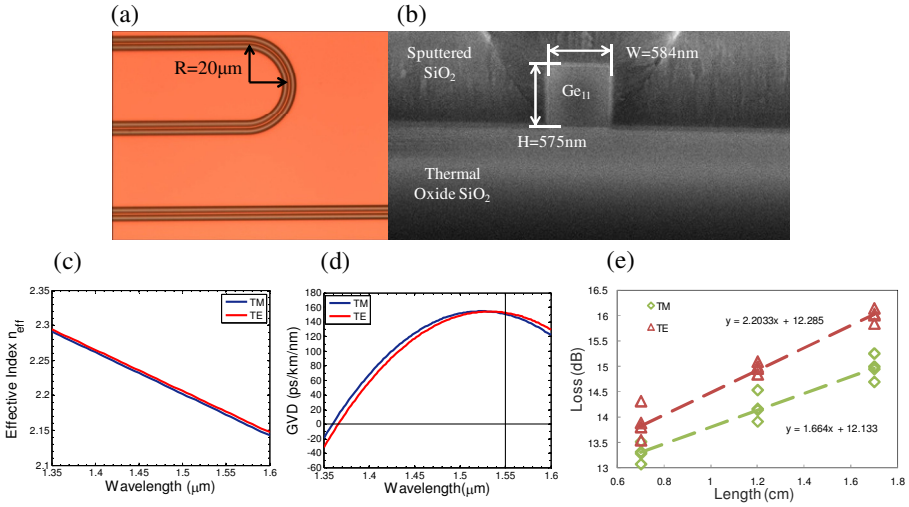

Fig. 2. (a) An optical micrograph shows the bends which are part of the "snakes" used to increase the length of the Ge_{11} nanowires for loss measurements. The radius is 20μm. (b) An SEM cross sectional image of the square Ge_{11} nanowires buried in SiO_2 cladding. The width was measured to be 584nm and height 575nm. (c) The effective index of 585nm × 575nm nanowires. (d) The GVD of 585nm × 575nm nanowires. (e) The propagation loss measured by cut-back method. The green diamonds are for TM and red triangles for TE modes.

An advantage of using SiO_2 as a cladding is that there are no additional losses due to cladding absorption. In our previous work, As_2S_3 rib waveguide were generally clad with a UV cured polysiloxane inorganic polymer glass (IPG). However, it is found that the cured IPG has an absorption band from 1375nm to 1470nm with an dip of 2.5dB/cm and a very strong absorption band after 1620nm with the maximum absorption down to −32dB/cm at 1675nm, as shown in Fig. 3(a). Therefore, in a dispersion engineered waveguide where a significant part of the field penetrates the cladding, additional losses are present due to C-H and O-H overtone absorptions. We measured the transmission spectrum of a 6.5cm long, 2μm × 0.85μm As_2S_3 rib waveguide with the IPG cladding using a super-continuum generated by passing 7ps pulses from a mode-locked Nd:YVO_4 laser through a photonic crystal fiber. The results are shown in Fig. 3(b). The loss increased by 8dB at the strongest IPG absorption peak leading poor performance in the L-band. Since the SiO_2 cladding does not show any significant absorption in the telecommunications bands these losses can be eliminated. Figure

#167778 - $15.00 USD Received 1 May 2012; revised 22 May 2012; accepted 24 May 2012; published 1 Jun 2012

3 (c) shows the transmission spectrum of the Ge_{11} P-I nanowires. The transmission spectrum is essentially flat from 1250nm to 1700nm with no extra losses observed.

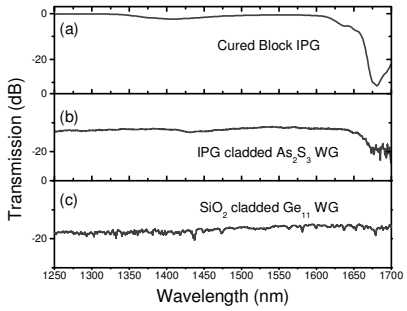

Fig. 3. (a) Transmision spectrum of cured IPG. 3(b) transmission spectrum of IPG clad As_2S_3 rib waveguide. (c) Transmission of SiO_2 clad Ge_{11} P-I nanowires.

3. Polarization independent FWM and Supercontinuum generation

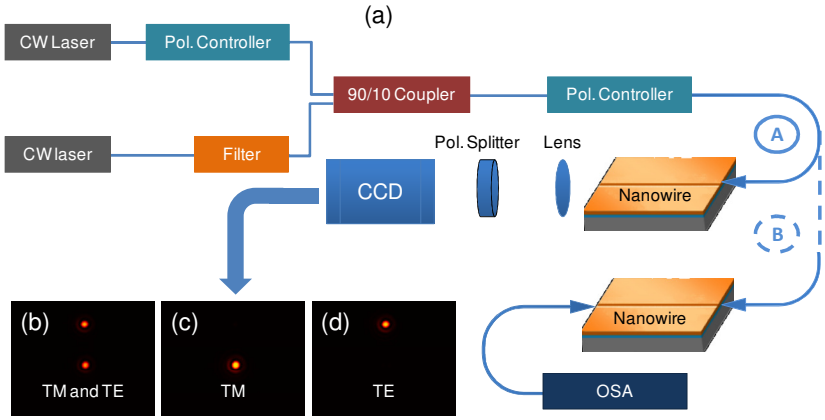

Fig. 4. Experimental set up. The lower image shows how the polarization state was set to TM or TE modes by imaging the waveguide output though a Wollaston prism onto an InGaAs camera.

Since P-I Ge_{11} nanowires have many applications in all-optical processing of telecommunication signals involving FWM, it is important to demonstrate P-I FWM in these nanowires. Because the device length is very short, it is difficult to measure GVD directly. However, the bandwidth of FWM is determined by the GVD through the phase matching condition, and hence we can evaluate differences in GVD by measuring the FWM spectrum. The experimental set up is shown is Fig. 4(a). Here 4ps pulses from a mode-locked fibre laser at a repetition rate of 10MHz acted as a pump at 1554.7nm. The pump was combined with a tunable CW probe signal using a 10/90 coupler. Two polarization controllers were added to set the polarization state to either the TM or TE mode. Lensed fibres producing a beam with a diameter of 2.5µm were used to couple light in and out of the nanowires. In order to monitor the polarization of the beam, a x10 objective lens was used to image the light at the output onto an InGaAs CCD camera through a Wollaston prism which separated the TM and TE polarizations vertically in the image plane as shown in Fig. 4 (b), 4(c) and 4(d). Figure 4(b) shows a mixed polarized state with equal power on both TM (bottom) and TE modes (top). Figures 4(c) and 4(b) show linear polarization in the TM and TE modes respectively.

#167778 - $15.00 USD Received 1 May 2012; revised 22 May 2012; accepted 24 May 2012; published 1 Jun 2012

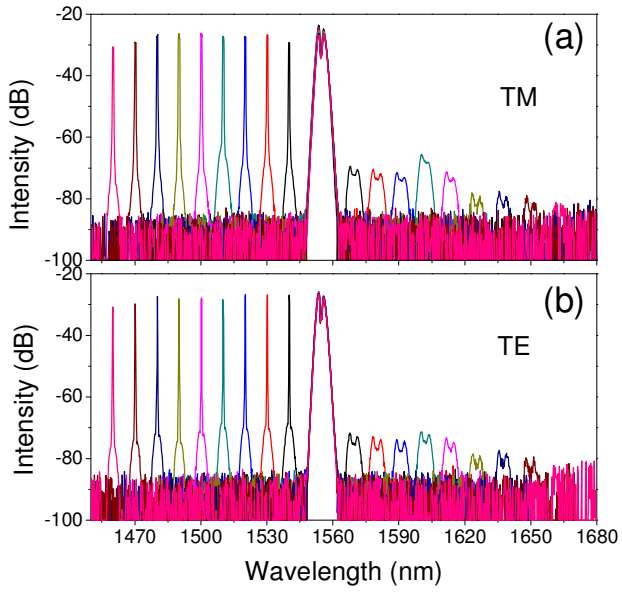

Fig. 5. FWM results for TM and TE modes. A pulsed pump was launched into the waveguide along with a low power CW probe beam. The idler output on the long wavelength side was measured a function of probe wavelength. (a) TM mode. (b) TE mode

In the experiment, the pump that was coupled into 7mm long nanowires had a peak power of 2.8W and was combined with a CW probe with a power of about 10μW. By tuning the wavelength of the probe beam, FWM was obtained for both TE and TM modes over a bandwidth of more than 180nm as shown in Fig. 5. The increase in the FWM signal around 1602nm is due to a contribution from stimulated Raman scattering [18, 23]. As shown in [18, 23] near the Raman peak, which in this material lies between 5 and 10THz below the pump frequency, the FWM conversion is modulated by the real part of the Raman response function. This causes a dispersion-like modulation of the conversion efficiency which first rises as the Raman peak is approached before dropping markedly and finally recovering to around 50%-70% of that for small frequency shifts before finally decreasing as the limits of phase matching are reached. The similar behavior observed for both TM and TE modes indicates that they have a very similar GVD confirming P-I dispersion.

To be more specific, we calculated the FWM spectrum by solving the nonlinear Schrödinger equation shown below using the split-step Fourier method:

$$\frac{\partial}{\partial z}A(z,t) = -\frac{\alpha}{2}A + \sum_{m\geq 2}\frac{i^{m+1}\beta_m}{m!}\frac{\partial^m A}{\partial t^m} + i\left(\gamma + i\frac{\alpha_2}{2A_{eff}}\right)\left(1+\frac{i}{\omega_0}\frac{\partial}{\partial t}\right)\left(A(z,t)\int_{-\infty}^{\infty}R(t')\left|A(z,t-t')\right|^2 dt'\right), \quad (1)$$

where A is the electric field amplitude, α = 1.67 dB/cm for TM and 2.33 dB/cm for TE is the linear loss of the waveguide. β_m is the mth order dispersion with the GVD calculated at 155ps/km/nm as shown in Fig. 2, α_2 = 9.3 × 10^{-14}m/W is the two-photon absorption coefficient and γ is nonlinear coefficient of 130W^{-1}m^{-1} for the square Ge_{11} nanowires. $R(t)$ =

#167778 - $15.00 USD Received 1 May 2012; revised 22 May 2012; accepted 24 May 2012; published 1 Jun 2012

$(1-f_R)\sigma(t) + f_R h_R(t)$ is the response function, including the Raman contribution $h_R(t)$ *and* $f_R = 0.12$ is the fractional Raman contribution.

We compared the conversion to the idler determined from the measurement with the simulation and obtained a good fit as shown in Fig. 6. According to both the experiments and modeling the conversion for the TE mode was about 0.5dB lower than that for the TM mode. This difference is mainly due to the different propagation losses of the TM and TE modes. Figure 6 clearly shows modulation of the FWM conversion around the Raman peak confirming the predictions in [18, 23]. To our knowledge, this is first experimental observation confirming the influence of $Re[h(\omega)]$ on FWM in a chalcogenide waveguide.

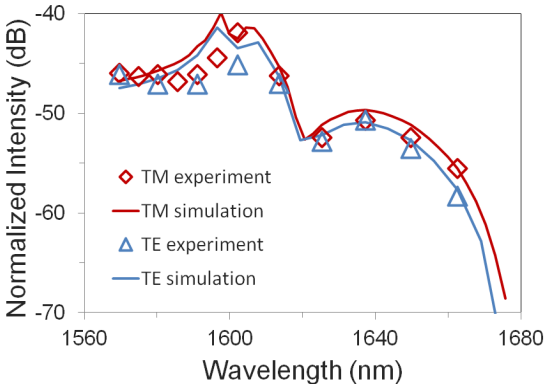

Fig. 6. Calculated (solid lines) and measured FWM conversion efficiency as a function of idler wavelength for TE (red) and TM (blue) modes.

Another important nonlinear process that is sensitive to the sign and magnitude of the dispersion is super-continuum (SC) generation. This was achieved using a 12mm long P-I nanowire pumped with 1ps duration pulses for both TM and TE modes as show in Fig. 7 (a). The power required to generate SC was slightly different for TE and TM modes due to the different losses and was ≈31W for the TM mode and 33W for the TE mode. Although the power required for SC was different, the spectra for both TM and TE modes were very similar. SC is a very complicated process involving self phase modulation, cross phase modulation, FWM, soliton fission, Raman scattering, etc, but the similarity in the SC spectrum indicates that these square Ge_{11} nanowires had not only similar GVD but also similar higher order dispersions. We simulated the SC spectrum using the split-step Fourier method for both TM and TE polarization for different peak powers and the results are shown in Figs. 7(b) and 7(c) respectively. The simulation results fit the measured spectra extremely well and also predict the measured difference in threshold power for generating SC for the two polarizations. According to the simulations, the SC extended over almost one octave from 1100nm to 2100nm. To our knowledge, this is the shortest glass waveguide ever to be used for broadband SC generation which indicates it should be possible to fabricate very compact P-I light sources on a photonic chip.

#167778 - $15.00 USD Received 1 May 2012; revised 22 May 2012; accepted 24 May 2012; published 1 Jun 2012

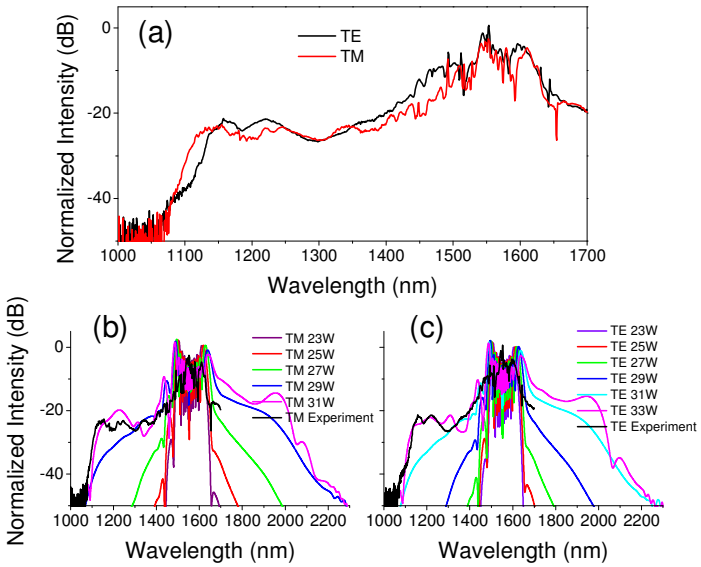

Fig. 7. 7(a) measured SC spectra for TE and TM modes. 7b, 7c, supercontinuum spectra for different pump powers calculated using the split-step Fourier method compared with the measured spectra.

Conclusion

We have shown that it is possible to fabricate highly nonlinear chalcogenide glass nanowires that offer polarization independent operation for nonlinear process such as FWM and super-continuum generation. The small residual PDL is likely to be due to roughness of the etched vertical sidewalls that has a bigger effect on the TE mode. It is possible that the PDL could be reduced by evaporating a thin Ge_{11} overcoat after etching as this has been previously shown to reduce sidewall losses by smoothing high spatial frequency roughness [24, 25]. From our experimental results we achieved a structure with very small polarization dependent dispersion and this should open up the possibilities of achieving FWM with a randomly polarized input made possible with a pair of orthogonally-polarized pumps [26]. To our knowledge this represents the first report of polarization independent nonlinear processing in an optical nanowire.

Acknowledgment

This research was conducted by the Australian Research Council Centre of Excellence for Ultrahigh Bandwidth Devices for Optical Systems (project CE110001018). The device fabrication was partially supported by the facilities of the Australian National Fabrication Facility (ANFF).

#167778 - $15.00 USD Received 1 May 2012; revised 22 May 2012; accepted 24 May 2012; published 1 Jun 2012